J Supercond Nov Magn (2017) 30:1727–1736
DOI 10.1007/s10948-017-3982-z

ORIGINAL PAPER

The Effects of Structural, Thermal, and Magnetic Properties of Hexylbenzene-Doped MgB_2 Superconductor

Hasan Ağıl[1] · Erhan Aksu[2] · Selçuk Aktürk[3] · Ali Gencer[4]

Received: 24 November 2016 / Accepted: 5 January 2017 / Published online: 26 January 2017

Abstract The effects of the amount of hexylbenzene additive ($C_{12}H_{18}$) on the structural, thermal, and magnetic properties of MgB_2 superconductor are examined in this study. Pure and hexylbenzene-doped MgB_2 bulk samples were produced with in situ solid-state reaction method. X-ray diffraction patterns of MgB_2 doped with MgB_2 and hexylbenzene at different ratios were determined to have MgB_2 as the main phase and consisted of a small amount of MgO. Pure and different ratios of hexylbenzene-doped Mg and B starting powders were heat-treated by a differential scanning calorimeter between room temperature and 800 °C. It was determined from the differential scanning calorimetry curves obtained that the first exothermic peak pointed the MgB_2 phase emerging with a solid–solid (Mg–B) reaction, and this temperature shifted towards the low temperatures as the hexylbenzene addition rates increased. It was observed that there was dependency to the applied field in all samples from the ac susceptibility measurements as a function of the temperature in pure and hexylbenzene-doped MgB_2 superconductor materials, and shift towards the lower temperatures in T_c, superconducting transition temperature, with increasing content. It was observed that the changes occurred in in-phase (χ') and out-off-phase (χ'') components of ac susceptibility both weakened the MgB_2 phase structure of hexylbenzene content and, as a result of this, led to changes in the pinning mechanism.

Keywords MgB_2 bulk · Flux pinning · Carbon addition

1 Introduction

When a MgB_2 superconductor is compared with Nb–Ti and Nb_3Sn, it is a promising material for power and medical applications because of its high critical temperature [1]. The cost of MgB_2 raw materials is lower than that of presently used Nb–Ti and Nb_3Sn conductors. Consequently, it has been believed that the MgB_2 superconductor has potential for industrial applications, in particular in the field of medical technology, where superconducting MRI magnets are used. However, the critical current density (J_c) of pure MgB_2 significantly decreases with an increasing external magnetic field due to its poor flux pinning properties.

A significant improvement of the electromagnetic properties in MgB_2 can be achieved through doping of carbon-containing compounds, such as SiC [2–4], C [5, 6], carbon nanotubes [7], aromatic hydrocarbons [8, 9], and carbohydrates [10–12]. However, liquid additives are believed to be more effective due to the agglomeration problem of the most of the carbon compounds which are solid ones. For this reason, hexylbenzene ($C_{12}H_{18}$) which is a type of

✉ Hasan Ağıl
hasanagil@hakkari.edu.tr

1 Department of Material Science and Engineering, Faculty of Engineering, Hakkari University, Hakkari, Turkey

2 Technology Department, Sarayköy Nuclear Research and Training Centre, Turkish Atomic Energy Authority, 06983 Ankara, Turkey

3 Department of Physics, Faculty of Sciences and Letters, Muğla Sıtkı Koçman University, Kötekli, 48000 Muğla, Turkey

4 Center of Excellence for Superconductivity Research, Ankara University, Golbasi 50. Yil Yerleskesi, Golbasi, 06830 Ankara, Turkey

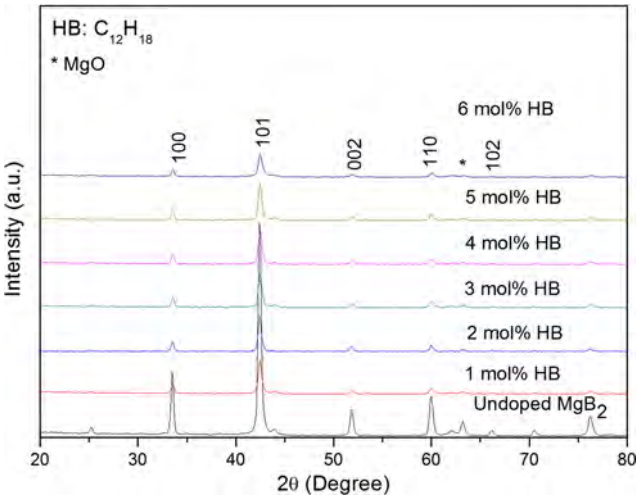

Fig. 1 X-ray diffraction patterns of pure and $C_{12}H_{18}$ added in MgB_2

liquid has been used as a carbon source in this work and its effects on structural, thermal, and magnetic properties of the hexylbenzene-doped MgB_2 superconductor have been investigated.

Table 1 The lattice parameters of all the samples

$C_{12}H_{18}$ (mol%)	*a*-axis lattice parameter (Å)	*c*-axis lattice parameter (Å)
0	3.08297	3.52624
1	3.07886	3.52180
2	3.08326	3.52598
3	3.07899	3.52359
4	3.07977	3.52365
5	3.06360	3.50921
6	3.08163	3.52474

2 Experimental Details

Polycrystalline MgB_2 bulk samples doped with different levels of hexylbenzene ($C_{12}H_{18}$) were prepared through a reaction in situ process. Mg powders (Alfa Aesar), amorphous boron (B) powders (Sigma-Aldrich), and hexylbenzene (Sigma-Aldrich) have been used as starting materials for this work. The amount of hexylbenzene added was between 1 and 6 mol %. The starting powders were mixed

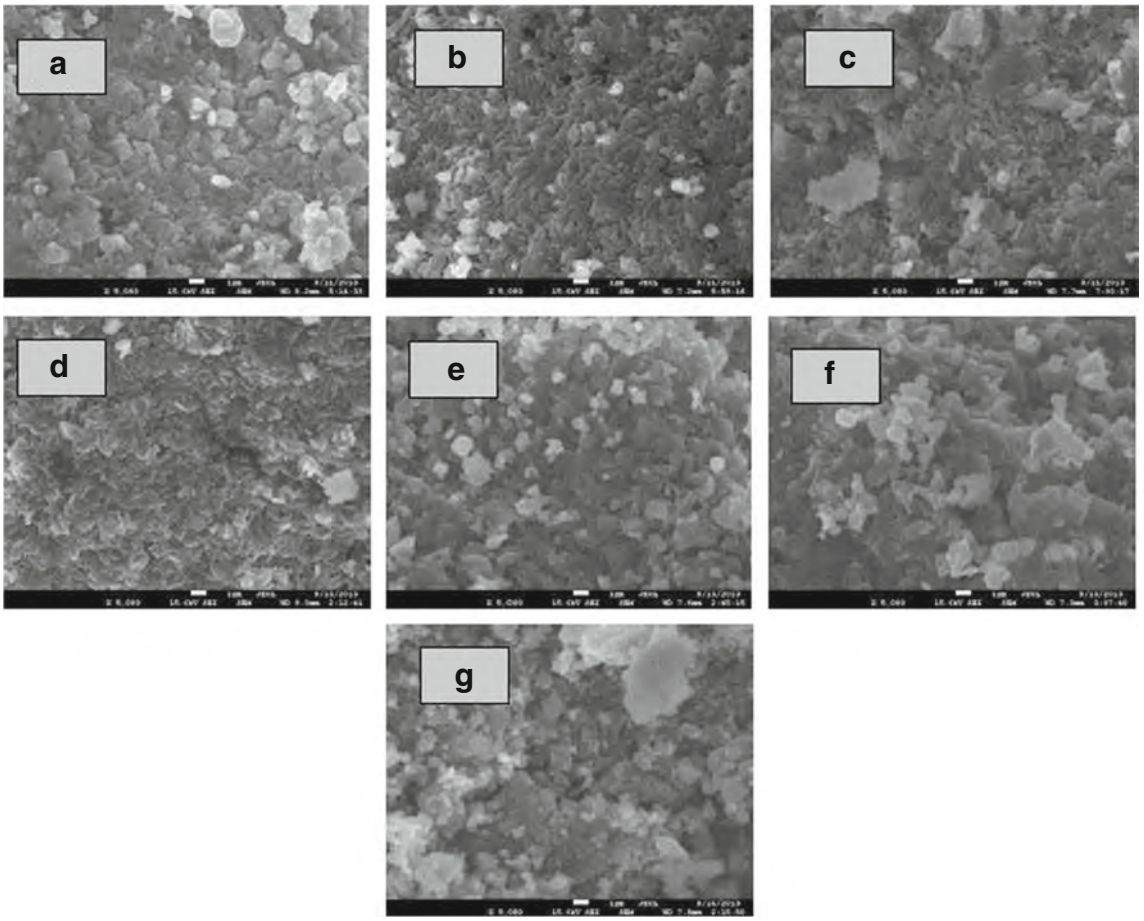

Fig. 2 **a**–**g** SEM images for the un-doped and doped samples

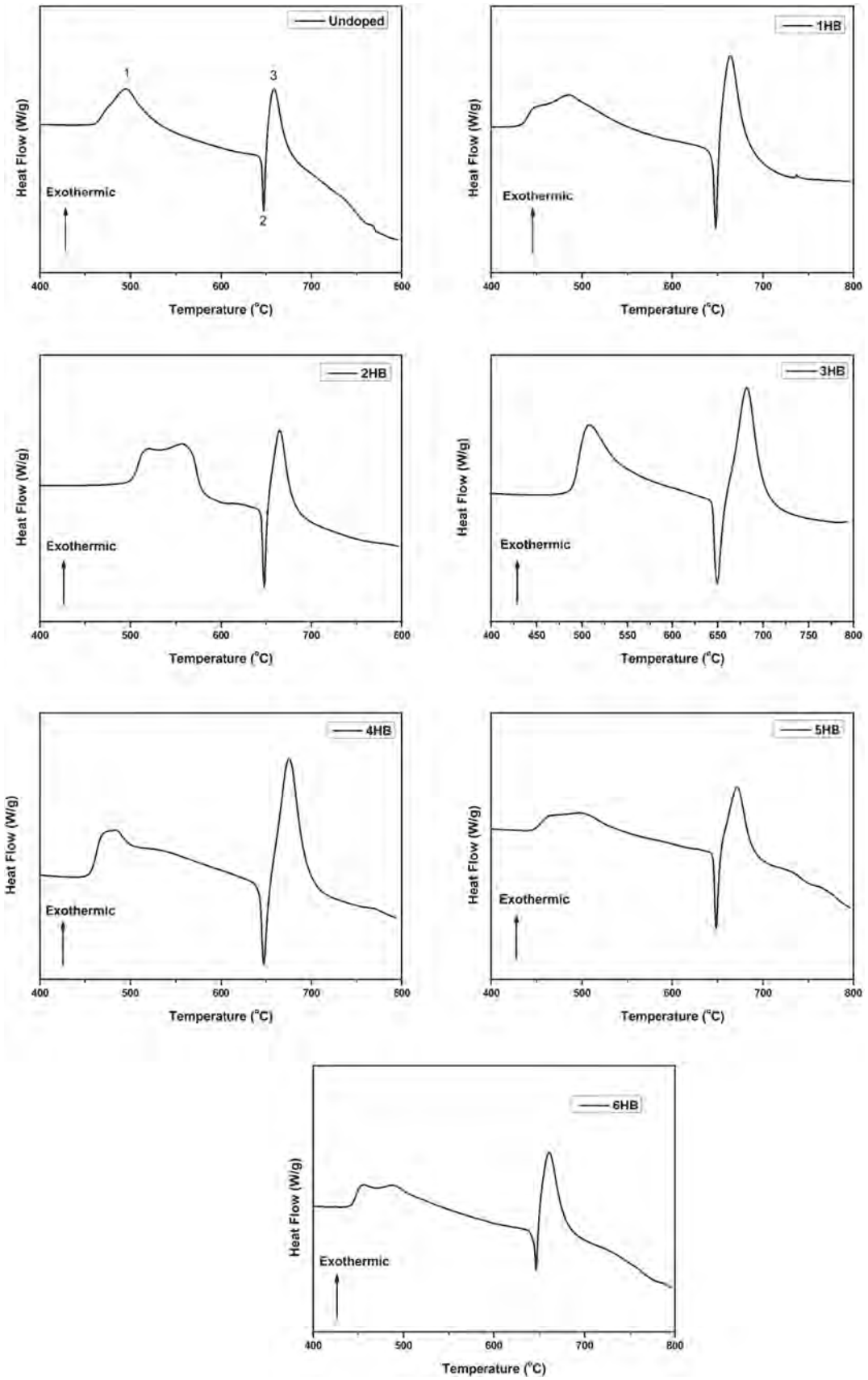

Fig. 3 DSC curves of the un-doped and hexylbenzene-doped MgB_2 samples

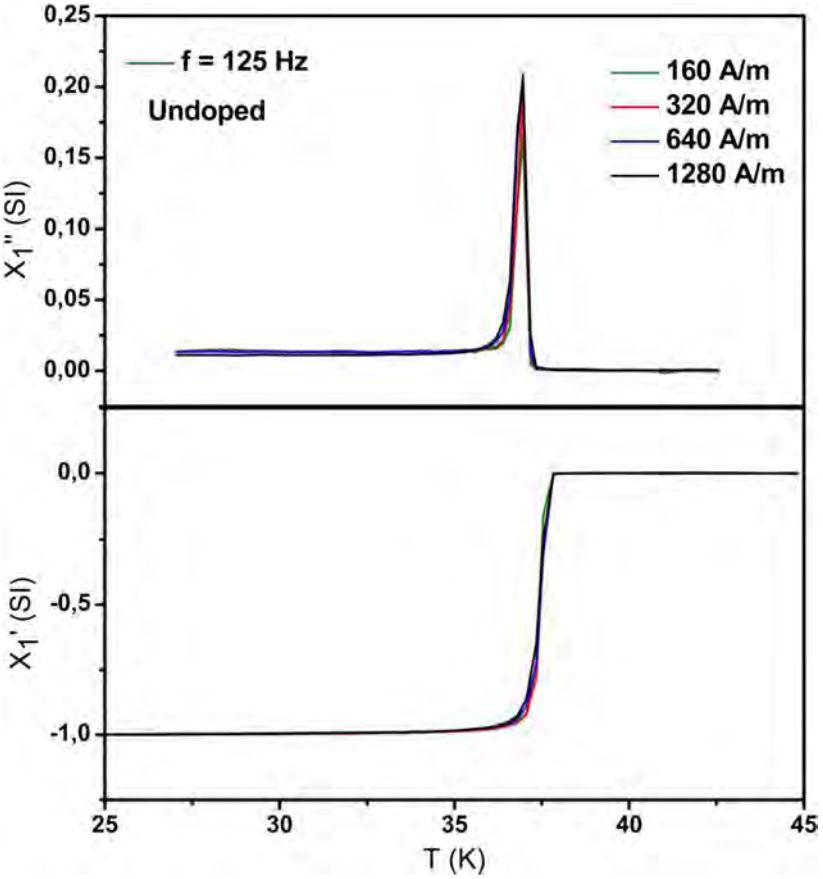

Fig. 4 AC susceptibility measurements for the pure MgB_2 samples

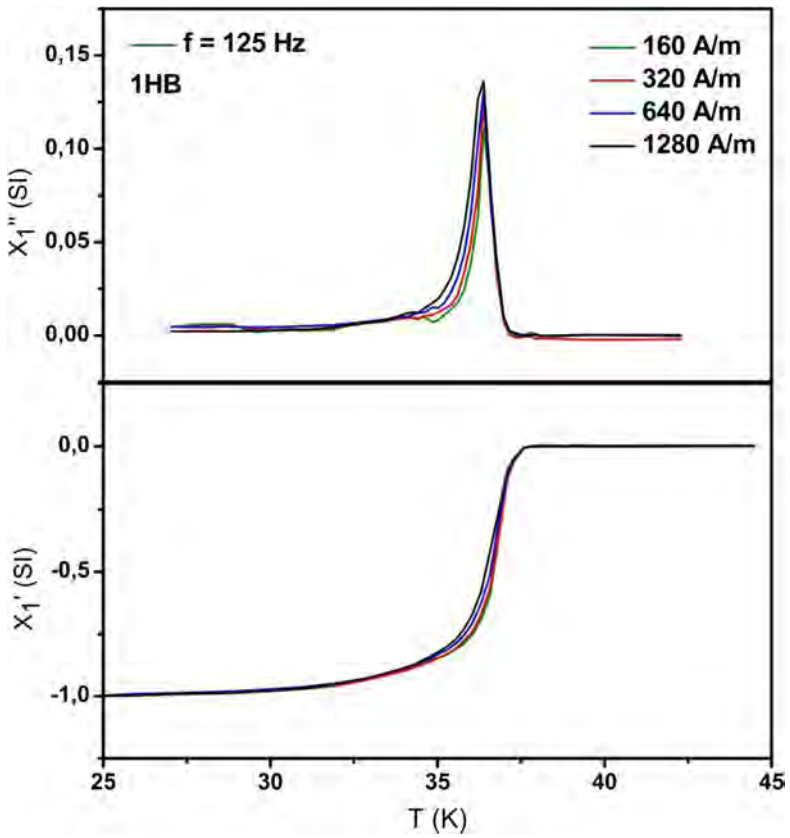

Fig. 5 AC susceptibility measurements for the 1 mol % $C_{12}H_{18}$-doped MgB_2 samples

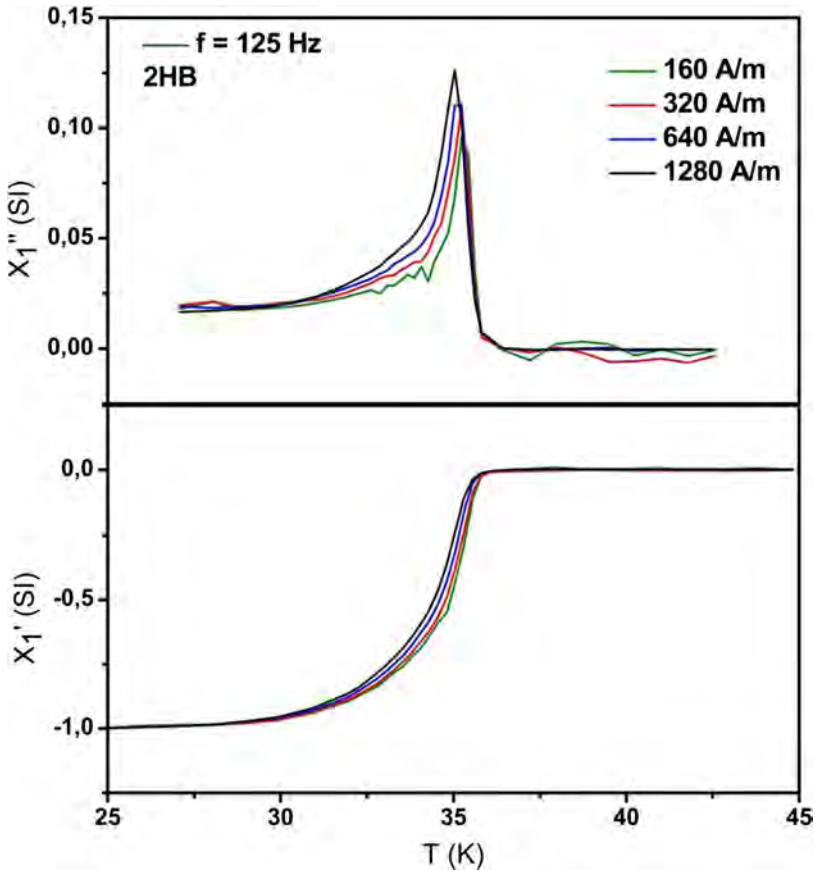

Fig. 6 AC susceptibility measurements for the 2 mol % $C_{12}H_{18}$-doped MgB_2 samples

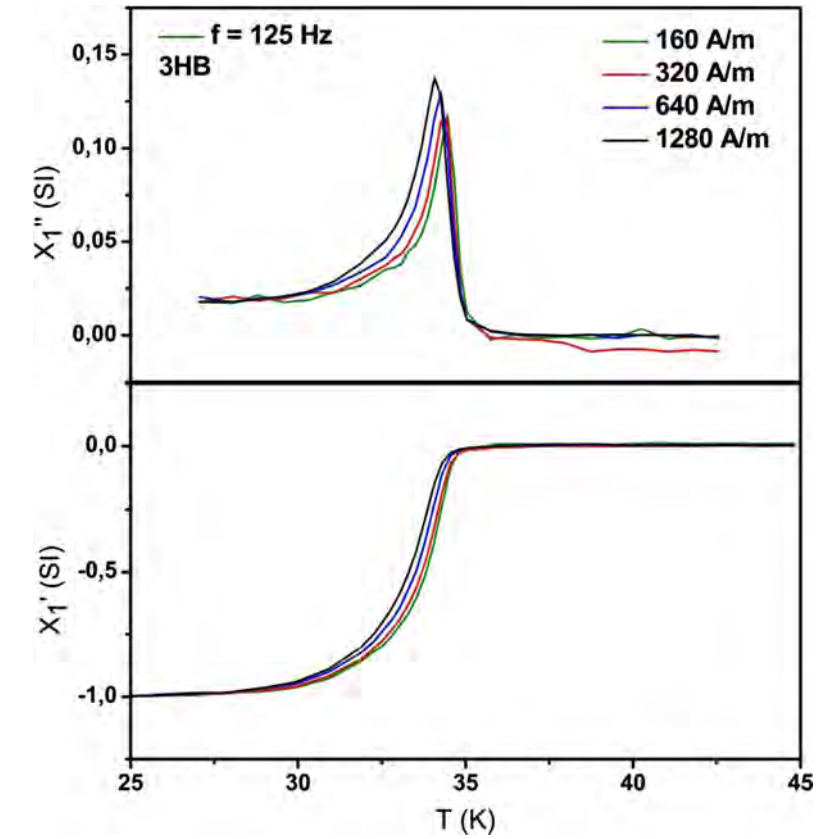

Fig. 7 AC susceptibility measurements for the 3 mol % $C_{12}H_{18}$-doped MgB_2 samples

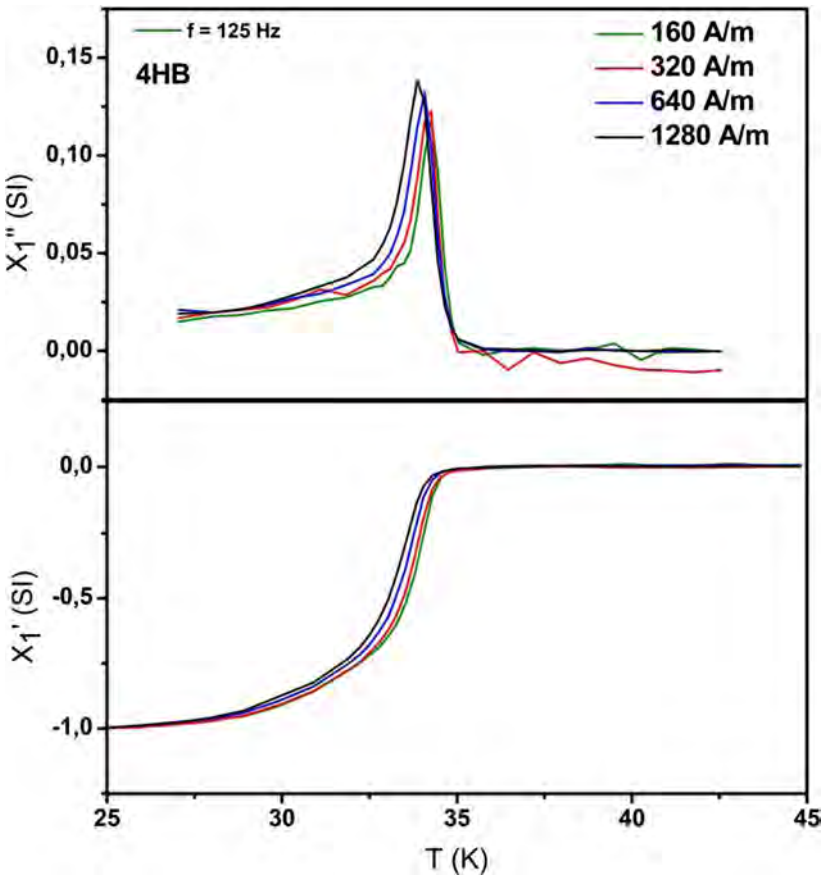

Fig. 8 AC susceptibility measurements for the 4 mol % $C_{12}H_{18}$-doped MgB_2 samples

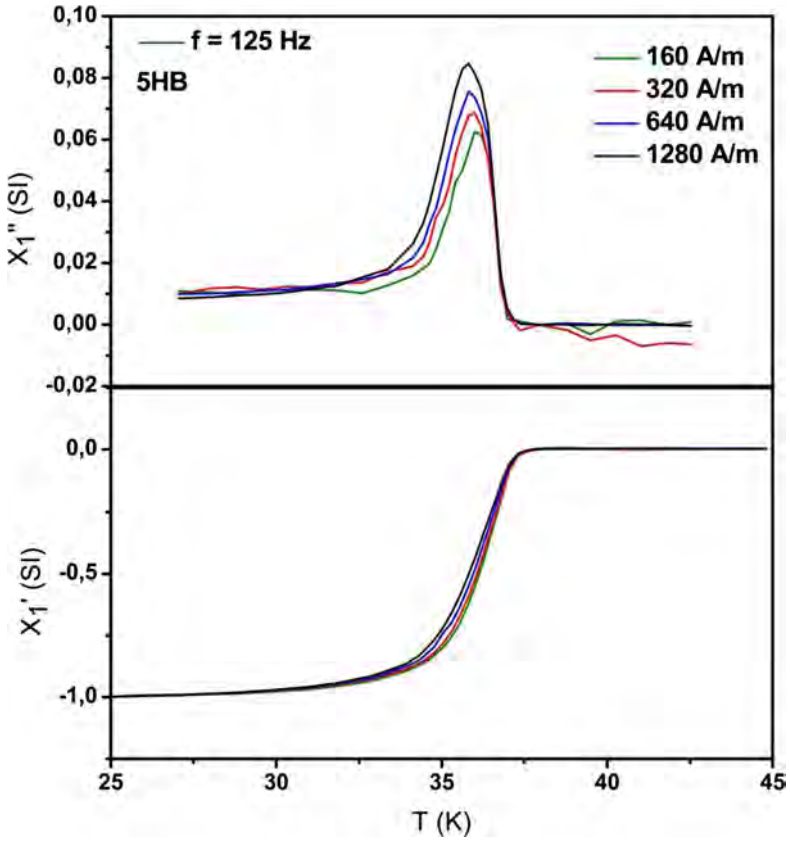

Fig. 9 AC susceptibility measurements for the 5 mol % $C_{12}H_{18}$-doped MgB_2 samples

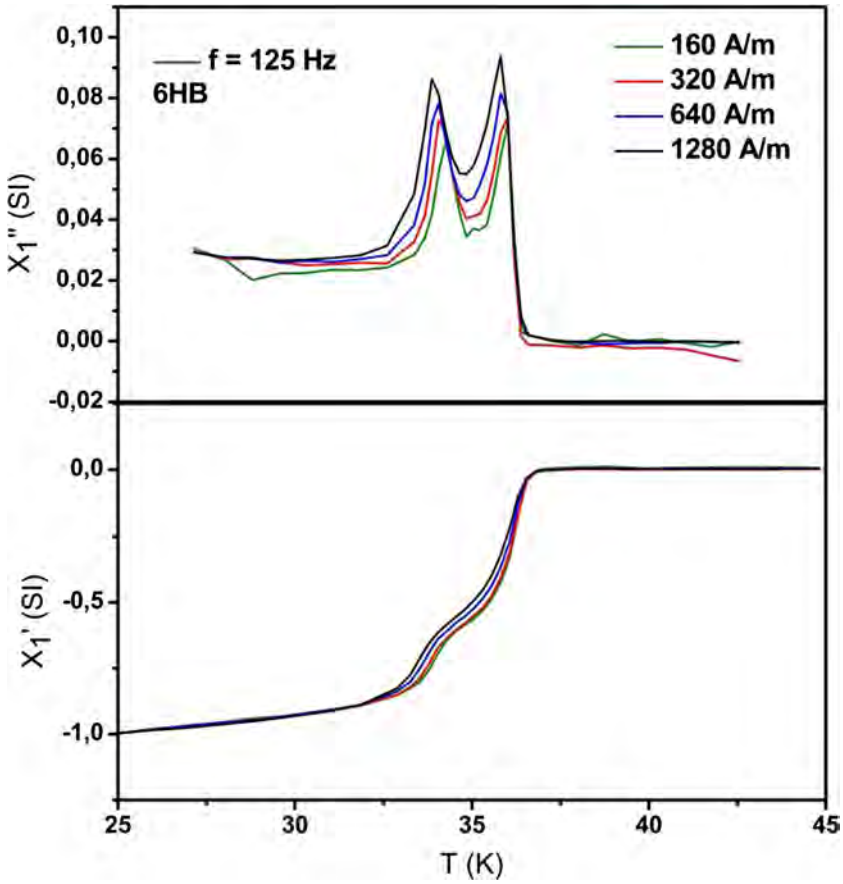

Fig. 10 AC susceptibility measurements for the 6 mol % $C_{12}H_{18}$-doped MgB_2 samples

for 5 h with a rotating speed of 150 rpm in the ball mill using a stainless steel ball and jar. The powder-to-ball weight ratio was selected to be 1:10. Then, milled powder was pressed into the pellet form. All samples were subjected to heat treatment for 1 h at 850 °C under Ar atmosphere in a stainless steel tube. The heating rate was 5 °C/min. The thermal characterization of the non-sintered powder samples was studied by thermal analysis techniques including thermogravimetry (TG) and differential scanning calorimetry (DSC) simultaneously. The DSC measurements were carried under the flow of high purity argon gas (200 ml/min) with a heating rate of 5 °C/min between the room temperature and 800 °C. In order to examine the morphology of all samples, the scanning electron microscope was used. X-ray diffraction measurements were carried out to determine the phase composition and the structural parameters by using the Rietveld refinement. The critical temperature (T_c) of all the samples was determined by the ac susceptibility measurements. Magnetic measurements were carried out at 5, 20, and 30 K by using a Quantum Design Physical Properties Measurement System (PPMS) in a time-varying magnetic field with a sweep rate 50 Oe/s and an amplitude of 8 T for pure, 1 mol %, and 6 mol % hexylbenzene-doped MgB_2 samples. The magnetic J_c of these samples was derived from the width of the magnetization loop by using Bean's model.

3 Results and Discussion

Figure 1 shows the XRD patterns of all the samples fabricated at different addition levels of $C_{12}H_{18}$. It can be observed that both the pure and the hexylbenzene-doped MgB_2 samples contain a well-developed MgB_2 phase with a small amount of MgO.

Table 2 The critical temperature (T_c) of the un-doped and $C_{12}H_{18}$-doped MgB_2 samples

$C_{12}H_{18}$ (mol %)	T_c (K)
0	37.89
1	37.67
2	36.05
3	35.05
4	34.99
5	37.44
6	36.94

The lattice parameters of all the samples calculated from the XRD data are shown in Table 1. It can be seen that the a-axis lattice parameter decreases for the pure and the hexylbenzene-doped samples. The c-axis lattice parameter is almost constant for both the un-doped and doped samples. The shrinkage of a-axis lattice parameter indicates the formation of defects caused by both carbon substitution into the boron sites and lattice strain in the crystal [13, 14].

Scanning electron microscopy (SEM) images for un-doped MgB_2 (a), MgB_2+ 1 mol % $C_{12}H_{18}$ (b), MgB_2+ 2 mol % $C_{12}H_{18}$ (c), MgB_2+ 3 mol % $C_{12}H_{18}$ (d), MgB_2+ 4 mol % $C_{12}H_{18}$ (e), MgB_2+ 5 mol% $C_{12}H_{18}$ (f), and MgB_2 + 6 mol% $C_{12}H_{18}$ (g) are shown in Fig. 2.

When the SEM images were analyzed, it was observed that all samples have a granular structure and are homogeneous. On the other hand, we have seen that all of the samples have a porous structure from the SEM images. The particle sizes of the samples were estimated to be below 1 μm.

The heat flow versus temperature curves are given in Fig. 3. When these curves are analyzed, there exist one endothermic peak and two exothermic peaks. The first exothermic peak can indicate the solid–solid reaction between Mg and B to form a MgB_2 phase. The endothermic peak is associated with the melting of the magnesium. The endothermic peak exists with a peak temperature between 647 and 651 °C. The second exothermic peak is due to the liquid–solid reaction between the liquid magnesium and the solid B as the magnesium is in liquid state at these temperatures.

When the measurements are examined, it is seen that the solid–solid reaction temperatures shifted to relatively low temperatures with hexylbenzene addition.

In Figs. 4, 5, 6, 7, 8, 9, and 10, we present the fundamental ac susceptibility measurements of pure and doped MgB_2

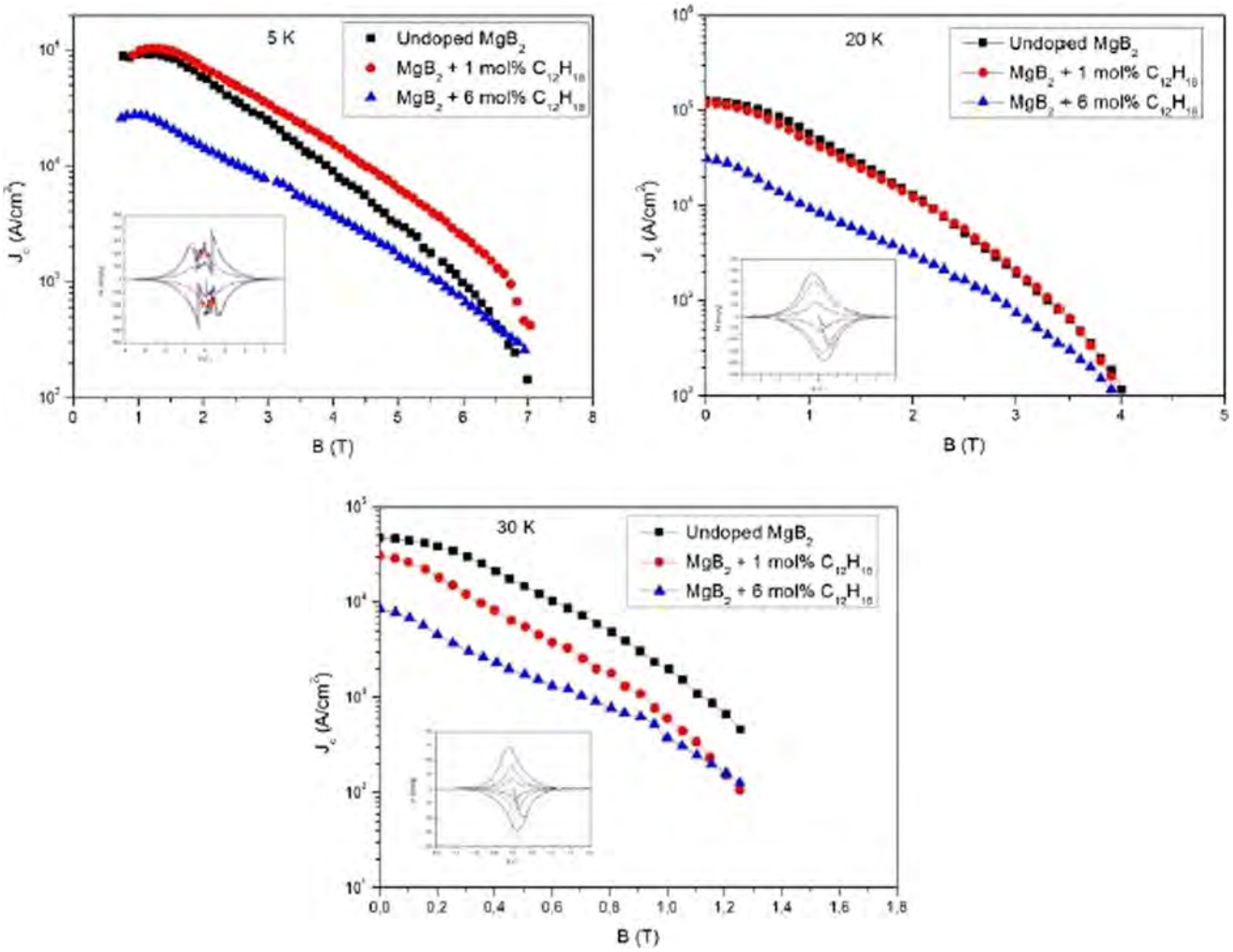

Fig. 11 $J_c(B)$ plots for the un-doped and doped samples at **a** 5 K, **b** 20 K, and **c** 30 K. The *insets* show the magnetization loops

samples for ac fields of 160, 320, 640, and 1280 A/m with a frequency of 125 Hz.

The onset of the transition temperature was obtained to be $T_{c,onset} = 37.8$ K for the pure sample. The T_c was depressed with increasing the additive level from 1 to 6 mol % (Table 2). In general, it is proposed that a possible substitution of C for B results in a depression of the critical temperature (T_c). However, the curves for in-phase (χ') and out-of-phase (χ'') versus temperature display a two-step process for the 6 mol % hexylbenzene-doped MgB_2 sample. In the first sharp drop, the particles in the superconductor are primarily regarded as a sign of starting to be superconducting. Another sharp drop which curving is relatively less sharp can be regarded as an indication that superconducting currents start to flow from particle to particle.

Figure 11a–c shows the magnetic field dependence of J_c for the un-doped, 1 mol %, and 6 mol % hexylbenzene-added MgB_2 samples together with the $M–H$ loops in the insets at 5, 20, and 30 K. The critical current densities (J_c) are calculated from magnetization (M) loops by using Bean's critical state model [15].

As the doping level increased, the self-field J_c decreased systematically. This behavior can be explained by the degradation of superconducting volume in the samples. Moreover, MgO which could be formed during the sintering of the samples could also affect the J_c values. However, the J_c for the 1 mol % hexylbenzene-doped sample is seen to improve in high magnetic field compared with the un-doped MgB_2 sample at 5 K.

The J_c values of the un-doped and the hexylbenzene-doped MgB_2 samples at 5, 20, and 30 K are given in Table 3.

It is well known that a flux jumping phenomenon has been a severe problem for the application of superconductors [16]. A thermal impulse occurs during the measurement and causes the decreasing of critical current density and allows a flux to penetrate as an avalanche process. In our samples, a complete flux jumping phenomenon was observed at the temperature of 5 K. The reason of flux jumping was given by Ref. [16]; since the magnetic diffusion rate becomes faster than thermal diffusion rate at low temperature, the magnetic flux abruptly moves to cause flux jumps.

Table 3 The J_c values of the un-doped and hexylbenzene-doped MgB_2 samples at 5, 20, and 30 K

$C_{12}H_{18}$ (mol%)	Temperature (K)	B (T)	J_c (A/cm^2)
0	5	7	1.4×10^2
1	5	7	4.2×10^2
6	5	7	2.6×10^2
0	20	0	1.2×10^5
1	20	0	1.18×10^5
6	20	0	3×10^4
0	30	0	4.7×10^4
1	30	0	3×10^4
6	30	0	8.5×10^3

4 Conclusion

In the present study, we have systematically investigated the effects of $C_{12}H_{18}$ doping on the MgB_2 phase formation, lattice parameters, thermal properties, critical temperature (T_c), and critical current density (J_c). All of the samples were produced with an in situ solid-state reaction method. The decreases in the a-axis length and T_c due to the carbon substitution were observed in the $C_{12}H_{18}$-doped samples. From the SEM images it was observed that all samples have a granular structure and are homogeneous. The T_c was depressed with increasing the additive level from 1 to 6 mol % from the ac susceptibility measurements. Compared to pure MgB_2 with 1 mol % $C_{12}H_{18}$-doped sample improve the J_c value in the high field region that was found to decrease whereas the T_c value. The 6 mol % $C_{12}H_{18}$-doped sample had a lower J_c compared to pure sample was observed.

Acknowledgments This work was supported by the Research Fund of Hakkari University, Hakkari, Turkey, under grant contract no. MF2014BAP2, and by the Republic of Turkey, Ministry of Development, under the project number 2010K120520.

References

1. Nagamatsu, J., Nakagawa, N., Muranaka, T., Zenitani, Y., Akimitsu, J.: Nature **410**, 63 (2001)
2. Dou, S.X., Soltanian, S., Horvat, J., Wang, X.L., Zhou, S.H., Ionescu, M., Liu, H.K., Munroe, P., Tomsic, M.: Appl. Phys. Lett. **81**, 3419–3421 (2002)
3. Kumakura, H., Kitaguchi, H., Matsumoto, A., Hatekayama, H.: Appl. Phys. Lett. **84**, 3669–3671 (2004)
4. Sumption, M.D., Bhatia, M., Dou, S.X., Rindfliesch, M., Tomsic, M., Arda, L., Ozdemir, M., Hascicek, Y., Collings, E.W.: Supercond. Sci. Technol. **17**, 1180–1184 (2004)
5. Wilke, R.H.T., Bud'ko, S.L., Canfield, P.C., Finnemore, D.K., Suplinskas, R.J., Hannahs, S.T.: Phys. Rev. Lett. **92**, 217003 (2004)
6. Yeoh, W.K., Kim, J.H., Horvat, J., Xu, X., Qin, M.J., Dou, S.X., Jiang, C.H., Nakane, T., Kumakura, H., Munroe, P.: Supercond. Sci. Technol. **19**, 596–599 (2006)
7. Kim, J.H., Yeoh, W.K., Qin, M.J., Xu, X., Dou, S.X.: J. Appl. Phys. **100**, 013908 (2006)
8. Yamada, H., Hirakawa, M., Kumakura, H., Kitaguchi, H.: Supercond. Sci. Technol. **19**, 175–177 (2006)
9. Babaoğlu Meral, G., Serap, S., Özlem, Ç., Hasan, A., Ercan, E., Md, H., Shahriar, A., Ekrem, Y., Ali, G.: J. Magn. Magn. Mater. **324**(21), 3455–3459 (2012)

10. Kim, J.H., Zhou, S., Hossain, M.S.A., Pan, A.V., Dou, S.X.: Appl. Phys. Lett. **89**, 142505 (2006)
11. Hossain, M.S.A., Kim, J.H., Xu, X., Wang, X.L., Rindfleisch, M., Tomsic, M., Sumption, M.D., Collings, E.W., Dou, S.X.: Supercond. Sci. Technol. **20**, L51–L54 (2007)
12. Ağl, H., Çiçek, Ö., Ertekin, E., Motaman, A., Hossain, M.S.A., Dou, S.X., Gencer, A.: J. Supercond. Novel Magn. **26**(5), 1525–1529 (2013)
13. Kazakov, S.M., Puzniak, R., Rogacki, K., Mironov, A.V., Zhigadlo, N.D., Jun, J., Soltmann, C.h., Batlogg, B., Karpinski, J.: Phys. Rev. B **71**, 024533 (2005)
14. Senkowicz, B.J., Giencke, J.E., Patnaik, S., Eom, C.B., Hellstrom, E.E., Larbalestier, D.C.: Appl. Phys. Lett. **86**, 202502 (2005)
15. Bean, C.P.: Rev. Mod. Phys. **36**, 31–39 (1964)
16. Kimishima, Y., Takami, S., Okuda, T., Uehara, M., Kuramoto, T., Sugiyama, Y.: Phys. C **281-285**, 463–465 (2007)